Nonlinear Dyn (2012) 67:2255–2265
DOI 10.1007/s11071-011-0143-y

ORIGINAL PAPER

A new fundamental diagram theory with the individual difference of the driver's perception ability

Tieqiao Tang · Chuanyao Li · Haijun Huang · Huayan Shang

Received: 14 February 2011 / Accepted: 20 June 2011 / Published online: 13 July 2011

Abstract Based on the driver's individual difference of the driver's perception ability, we in this paper develop a new fundamental diagram with the driver's perceived error and speed deviation difference. The analytical and numerical results show that the speed-density and flow-density data are divided into three prominent regions. In the first region, the speed-density and flow-density data are scattered around the equilibrium speed-density and flow-density curves of the classical fundamental diagram theory, where the widths of these scattered data are very narrow and slightly increase with the real density (i.e., the scattered data appear as two thicker lines); the running speed is approximately equal to the free flow speed and the real flow approximately linearly increases with the real density. In the second region, the speed-density and flow-density data are scattered widely in a two-dimensional region, but the shapes of these widely scattered data are related to the properties of the driver's perceived error and speed deviation difference. In the third region, the scattered speed-density and flow-density data appear but these scattered data will quickly degenerate into the equilibrium speed-density and flow-density curves with the increase of the real density. Finally, the numerical results illustrate that the new fundamental diagram theory also produces the F-line, U-line, and L-line. The shapes of the scattered data, F-line, U-line, and L-line are relevant to the properties of the driver's perceived error and speed deviation difference. These results are qualitatively accordant with the real traffic, which shows that the new fundamental diagram theory can better describe some complex traffic phenomena in the real traffic system. In addition, the above results can help us to further explain why the widely scattered speed-density and flow-density data appear in the real traffic system and better understand the effects of the driver's individual difference on traffic flow.

Keywords Fundamental diagram theory · Driver's perceived error · Driver's speed deviation difference · Equilibrium flow

T. Tang (✉) · C. Li
School of Transportation Science and Engineering, Beihang University, Beijing 100191, China
e-mail: tieqiaotang@buaa.edu.cn

T. Tang · H. Huang
School of Economics and Management, Beihang University, Beijing 100191, China

H. Shang
Information College, Capital University of Economics and Business, Beijing 100070, China

1 Introduction

So far, serious traffic problems have attracted scholars to develop many traffic flow models to study various complex traffic phenomena [1]. Roughly speaking, the existing traffic flow theory can be divided into the

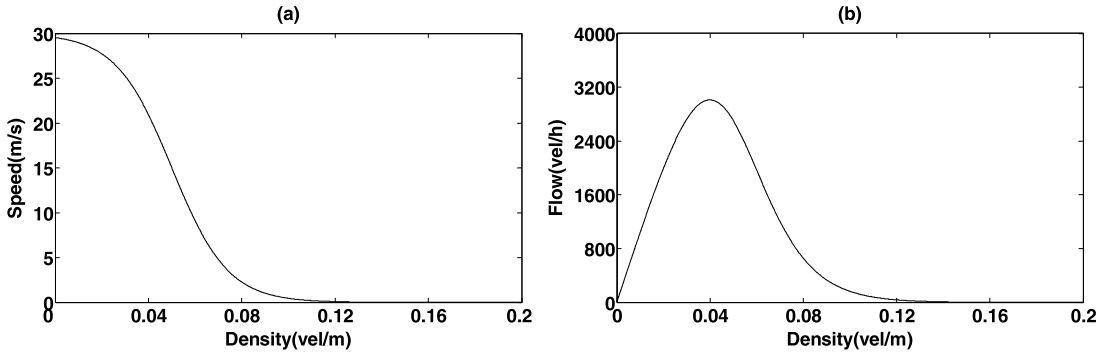

Fig. 1 The speed-density and flow-density relationships in the classical fundamental diagram theory

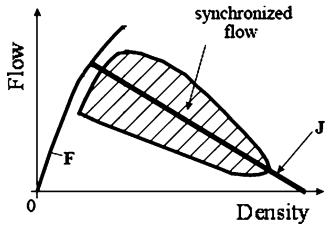

Fig. 2 The flow-density relationship in the three phase traffic flow theory [2]

three phase traffic flow theory [2–32] and the fundamental diagram theory [33–71]. The fundamental diagram theory assumes that there is always an equilibrium speed in the traffic system and that the equilibrium speed will decrease with density and that the flow will first increase then decrease with density (see Fig. 1); the three phase traffic flow theory thinks that the traffic system does not have the equilibrium speed and that traffic flow can be divided into free flow, synchronized flow, and widely moving traffic jam (see Fig. 2).

Based on the above theories, a new fundamental diagram theory with the driver's perceived error and speed deviation difference is proposed in this paper. The analytical and numerical results show that this new model is able to reproduce the effects of error and deviation difference on traffic flow and explain the widely scattered speed-density and flow-density data. In Sect. 2, the fundamental diagram theory and three phase traffic flow theory are reviewed. In Sect. 3, a new fundamental diagram theory is developed. In Sect. 4, the analytical deductions and numerical tests are carried out. Finally, conclusions and outlooks are summarized in Sects. 5 and 6.

2 Literature review

Kerner and his cooperators developed the three phase traffic flow theory based on many empirical data [2–25]. Kerner and his cooperators first found an almost stationary moving jam exists in the real traffic based on empirical data [3] and then proposed the definition of three qualitative different kinds of traffic: "free" traffic flow, "synchronized" traffic flow, and traffic jams [4]. Later, the transformation of the three traffic patterns are studied [5–10, 14, 18, 21, 24]. With the development of the theory, they found that many factors (e.g., ramp, merge bottlenecks) will produce the three phase traffic flow [2, 11–25] and many traffic phenomena are studied [11–13, 16, 19, 22]. The three phase traffic flow theory can reproduce and explain the widely scattered flow-density data in the real traffic system (see Fig. 3) from some specific perspectives, so it is popularly employed to explore the complex traffic phenomena that are difficultly explained by the classical fundamental diagram theory [26–32], e.g., phase transition of different traffic states [26, 28], impacts of driver performance [27, 31, 32] and bottleneck [30]. However, scholars later found that three phase traffic flow theory cannot completely explain the formation mechanisms of the widely scattered flow-density data [72–75]. For example, Helbing and his cooperators have explored the existing three phase traffic flow theory and compared the fundamental diagram theory with the three phase traffic flow theory [74, 75].

The classical fundamental diagram theory has been used to study the complex traffic phenomena from many different perspectives, such as the macroscopic model [33–37, 39–63, 66, 68–71] and microscopic model [38, 64, 65, 67]. However, the classical fundamental diagram theory cannot display or explain the

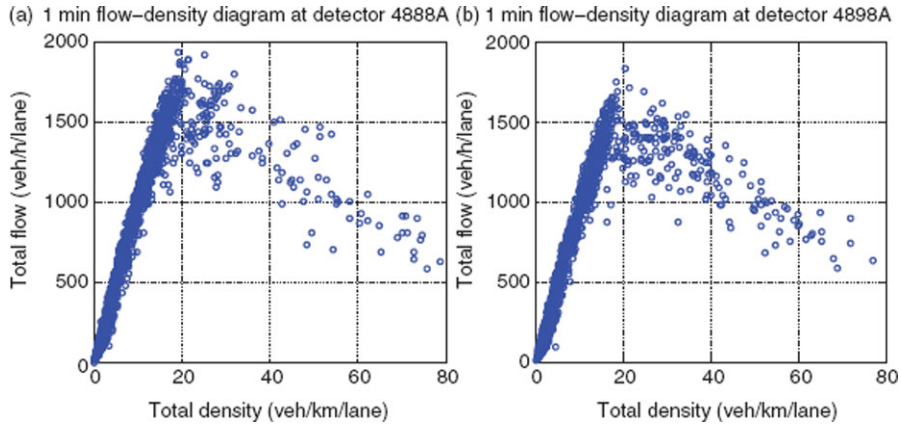

Fig. 3 One-minute empirical flow-density relationships of freeway M25 in England [76]

widely scattered data (see Fig. 3) because it did not consider the heterogeneity of vehicles, the stochastic factors, and others. In order to explore the widely scattered data, some new models were proposed based on many observed data and the formation mechanism of the widely scattered flow-density data can reasonably be explained from some specific perspectives (which have greatly enriched the fundamental diagram theory of traffic flow) [72–75, 77–80], but they cannot completely describe the stochastic factors since some stochastic factors were not explicitly considered yet. To overcome this drawback, Ngody [76, 81] developed a new multiclass first-order model and found the widely scattered data are resulted by the mixture of traffic flow and some stochastic factors. Yang and Peng [82] proposed an errorable car-following model that is more useful to design and evaluate an active safety vehicle system; Li et al. [83] presented a new LWR (Lighthill–Whitham–Richards) model with stochastic free flow speed. The above fundamental diagram theory can successfully explain some complex traffic phenomena, but they cannot be used to explore the effects of the driver's individual difference on traffic flow since they did not explicitly consider the factor. In this paper, we develop a new fundamental diagram theory based on the individual difference of the driver's perception ability and use it to study equilibrium flow.

3 Model

The classical fundamental diagram theory has been employed in the kinematic model, car-following model and dynamic model, where the classical kinematic model is the LWR model [33, 34]:

$$\rho_t + \big(\rho v_e(\rho)\big)_x = 0, \tag{1}$$

where ρ, $v_e(\rho)$, respectively, are the density and equilibrium speed. Equation (1) can reproduce the formation and propagation of shock and other complex phenomena, so scholars later proposed many extended LWR models from different perspectives [38, 43–45, 53, 56, 58, 66]. However, the LWR and its extensions cannot be used to describe the nonequilibrium traffic flow since its speed cannot deviate from $v_e(\rho)$. Thus, scholars later developed many high order models. The existing high order models can be divided into the DG (density-gradient) and SG (speed-gradient) models, where the classical DG one is the Payne model [35]:

$$\begin{cases} \rho_t + (\rho v)_x = 0, \\ v_t + v v_x = \dfrac{v_e - v}{\tau} - \dfrac{\upsilon}{\rho\tau}\rho_x, \end{cases} \tag{2}$$

where τ is the relaxation time and $\upsilon = -\frac{1}{2}v_e'(\rho)$ is the anticipation coefficient. Equation (2) can describe some nonequilibrium properties of traffic flow (stop-and-go, local cluster, etc.), so scholars developed another DG model from different perspectives [37, 40, 41, 46–50, 55, 62, 69–71]. The DG models can describe many complex traffic phenomena that the LWR model and its extensions cannot represent, but they will produce backward motion under some given conditions [84]. In order to conquer this drawback, Aw and Rascle [51, 59] proposed the first SG model and Zhang [60] extended it, but the two models did not

consider the relaxation term. Thus, Jiang et al. later developed another SG model [57], i.e.,

$$\begin{cases} \rho_t + (\rho v)_x = 0, \\ v_t + v v_x = \dfrac{v_e - v}{\tau} + c_0 v_x, \end{cases} \tag{3}$$

where c_0 is the propagation speed of small perturbation. Jiang et al. [57] found that (3) will not produce backward motion and it can describe some nonequilibrium properties of traffic flow (stop-and-go, local cluster, shock, rarefaction wave, etc.), so scholars developed another SG models from different perspectives [61, 68].

Equations (1)–(3) and their extensions can reproduce some complex traffic phenomena, but they cannot be employed to describe the motion of each vehicle. Thus, scholars proposed many car-following models [36, 39, 42, 52, 54, 63–65, 67], which can be reduced as follows:

$$\frac{\mathrm{d}v_n(t)}{\mathrm{d}t} = f\big(V\big(\Delta x_n(t), \ldots\big), v_n, \Delta v_n, \ldots\big), \tag{4}$$

where $v_n, \Delta x_n, \Delta v_n$ are respectively the speed, headway, and relative speed of the nth car, $V(\Delta x_n(t), \ldots)$ is the optimal speed which corresponds to the equilibrium speed in (1)–(3). Equation (4) explicitly considers the effects of some micro factors on each car's acceleration, so it can reproduce many micro phenomena.

The models [33–71] have many prominent differences, but they can be simplified as (1)–(4) from some different perspectives and all have an equilibrium solution $v_e(\rho)$ (ρ is the equilibrium density) or $V(\Delta x)$ ($V(\Delta x)$ is the optimal speed, Δx is the equilibrium headway).[1] Thus, we can obtain the equilibrium speed and flow, i.e.,

$$\begin{aligned} v_0 &= v_e(\rho_0), \\ q_0 &= \rho_0 v_e(\rho_0), \end{aligned} \tag{5}$$

where ρ_0, v_0, q_0 are respectively the equilibrium density, speed, and flow.

Thus, we can obtain the equilibrium speed-density and flow-density curves as long as we properly define $v_e(\rho)$ (see Fig. 1). However, the real flow-density data will be scattered widely in one two-dimensional region (see Fig. 3), so the models [33–71] cannot be used to describe the widely scattered data. In order to study the scattered data, some new models were proposed based on many observed data and the formation mechanism of the widely scattered flow-density data can reasonably be explained from some specific perspectives [72–75, 77–80], but they cannot be completely the stochastic factor because some stochastic factors were not explicitly considered yet. In order to further enrich the fundamental diagram theory, some new models with the stochastic factors were developed [76, 81–83], but they cannot be used to describe the effects of the driver's individual difference on traffic flow since they did not consider this factor. In fact, the driver's perception ability has the individual difference, so we must consider the individual difference when we study traffic flow. Hence, we can divide the driver's perceived density into the real density and the driver's perceived error, i.e.

$$\rho = \bar{\rho} + \varepsilon, \tag{6}$$

where $\rho, \bar{\rho}$ are respectively the driver's perceived density and the real density, ε is the driver's perceived error. The driver's perceived density will provide him an equilibrium speed $v_e(\rho)$, but the driver's running speed will often deviate from the expected equilibrium speed because of the driver's individual difference, i.e.,

$$\bar{v}(\rho) = v_e(\rho) + \eta, \tag{7}$$

where $\bar{v}(\rho)$ is the driver's running speed and η is the driver's speed deviation difference. Thus, we obtain a new fundamental diagram theory with the driver's perceived error and speed deviation difference, i.e.,

$$\begin{aligned} \bar{q} &= \bar{\rho} v_e(\bar{\rho} + \varepsilon) + \bar{\rho}\eta \\ &= \bar{\rho} v_e(\bar{\rho}) + \bar{\rho}\left(\varepsilon \frac{\mathrm{d}v_e(\bar{\rho})}{\mathrm{d}\bar{\rho}} + \eta\right) + \cdots, \end{aligned} \tag{8}$$

where $\bar{q}$ is the real flow. Since the new fundamental diagram theory has considered the individual difference of the driver's perception ability, it can better describe various complex phenomena in the real traffic system.

4 Numerical tests

In this section, we study the effects of the driver's perceived error and speed deviation difference on traffic

[1] Note: the optimal speed $V(\Delta x)$ corresponds to the equilibrium speed $v_e(\rho)$ of (1)–(3).

flow. In the real traffic system, the driver's perceived error ε often satisfies the following conditions:

(1) When the real density is very low, the driver can clearly see the number of cars in front of him. At this time, ε is so small that we can neglect it.
(2) With the increase of the real density, ε cannot be neglected since driver can neither clearly see the number of cars in front of him nor exactly measure his headway, and $|\varepsilon|$ will increase with the flow;[2] with the further increase of the real density, the headway will gradually turn so small that driver can exactly measure his headway, so $|\varepsilon|$ will gradually reduce to zero. Based on the relationship between the flow and density, we can obtain that $|\varepsilon|$ will first increase then gradually decrease to zero with the real density.

It seems more logical to define the speed deviation difference η as a decreasing function of the traffic density because this property has also been revealed in many observations. However, in the real traffic system, the speed deviation difference η is complex and related to many factors, such as the driver's individual difference (aggressive and conservative), the density, the equilibrium speed $v_e(\rho)$, the number of vehicles on the road, the complexity of the traffic information, the flow, etc. Therefore, we should use many observed data to define the quantitative relationship between the speed deviation difference η and the real density ρ.[3] Since we here focus on exploring the qualitative effects of the driver individual difference on the fundamental diagram, we only consider the impacts of the qualitative property of the speed deviation difference η on traffic flow in this paper.

In the real traffic system, the aggressive driver's speed deviation difference increases with v_e (ρ) since the room that makes him produce the deviation difference will increase with his perceived headway; the conservative driver's speed deviation difference decreases with $v_e(\rho)(-\eta$ increases with $v_e(\rho))$ since the conservative driver thinks that the traffic risk coefficient will increase with $v_e(\rho)$. Thus, we find that $|\eta|$ will increase with $v_e(\rho)$. In order to further quantify η, we here set

$$\omega = \frac{\eta}{v_e(\rho)}, \tag{9}$$

where ω is the driver's relative deviation difference about speed and $|\omega|$ will satisfy the following conditions:

(a) When ρ is very low, all the cars run approximately at the free flow speed. At this time, η is very small even if η exists, so we can approximately define $|\omega|$ as zero.
(b) When ρ is very high, $v_e(\rho)$ is very small. There is little room that provides driver to raise the speed deviation difference, so $|\omega|$ is so small that we can approximately define it as zero.
(c) When ρ is moderate, $|\omega|$ cannot be defined as zero since the traffic flow is very complex. But $|\omega|$ increases with the complexity of the traffic information and the traffic information becomes more complex with the increase of the flow, so $|\omega|$ will increase with the flow. Based on the relationship between the flow and the density, we obtain that $|\omega|$ will first increase then decrease with the perceived density.

In order to study the effects of ε, η on traffic flow, we must discuss the relationship between ε, η and the driver's individual difference, so we divide the drivers into the aggressive and conservative ones. As to the two kinds of drivers, ε, η have the following properties:

(a) The aggressive drivers often underestimate the real density and overestimate the system equilibrium speed, so ε, η satisfy $\varepsilon \leq 0, \eta \geq 0$.
(b) The conservative drivers often overestimate the real density and underestimate the system equilibrium speed, ε, η satisfy $\varepsilon \geq 0, \eta \leq 0$.

Thus, we can obtain the following proposition based on (8).

Proposition 1 *The aggressive drivers will enhance the running speed and real flow while the conservative drivers will reduce the running speed and real flow.*

Next, we study the effects of ε, η on equilibrium flow. Combining (8) with the properties of ε, η, we have:

[2] $|\varepsilon|$ increases with the complexity of traffic information and the traffic information turns more complex with the increase of the flow, so $|\varepsilon|$ will increase with the flow.

[3] We will in the future investigate this topic and use the exact speed deviation difference to further study the effects of the driver's individual difference on the fundamental diagram.

(i) ε, η have little effect on the running speed and real flow when the real density is very low. At this time, the running speed is approximately equal to the free flow speed and the real flow will approximately linearly increase with the real density; the speed-density and flow-density data are scattered around the equilibrium speed-density and flow-density curves of the classical fundamental diagram theory, where the widths of these scattered data are very narrow and slightly increase with the real density, i.e., these scattered data will appear as two thicker lines.

(ii) ε, η have great effects on the running speed and real flow when the real density is moderate. At this time, the running speed and real flow will produce oscillating phenomena; the speed-density and flow-density data will be scattered widely in a two-dimensional region, but the shapes of these scattered data are often relevant to the properties of ε, η.

(iii) ε, η have some effects on the running speed and real flow when the real density is very high, but these effects will quickly turn weak. At this time, the scattered speed-density and flow-density data appear but quickly reduce to the equilibrium speed-density and flow-density curves.

In order to study the quantitative effects of ε, η on the equilibrium flow, we should define ε, ω. But ε, ω have little qualitative effect on the following results, so we here define them as follows:

$$\varepsilon = \begin{cases} 0, & \text{if } 0 \le \bar{\rho} < \rho_{\mathrm{cr}}^1, \\ \lambda(-\frac{\varepsilon_{\max}}{(\rho_{\mathrm{cr}}^1 - \rho_{\mathrm{cr}}^2)^2}(\bar{\rho} - \rho_{\mathrm{cr}}^2)^2 + \varepsilon_{\max}), & \\ \quad \text{if } \rho_{\mathrm{cr}}^1 \le \bar{\rho} < \rho_{\mathrm{cr}}^2, & \\ \lambda(-\frac{\varepsilon_{\max}}{(\rho_{\mathrm{j}} - \rho_{\mathrm{cr}}^2)^2}(\bar{\rho} - \rho_{\mathrm{cr}}^2)^2 + \varepsilon_{\max}), & \\ \quad \text{if } \rho_{\mathrm{cr}}^2 \le \bar{\rho} \le \rho_{\mathrm{j}}, & \end{cases} \tag{10}$$

$$\omega = \begin{cases} 0, & \text{if } 0 \le \rho < \rho_{\mathrm{cr}}^3, \\ \xi(-\frac{\omega_{\max}}{(\rho_{\mathrm{cr}}^3 - \rho_{\mathrm{cr}}^4)^2}(\rho - \rho_{\mathrm{cr}}^4)^2 + \omega_{\max}), & \\ \quad \text{if } \rho_{\mathrm{cr}}^3 \le \rho < \rho_{\mathrm{cr}}^4, & \\ \xi(-\frac{\omega_{\max}}{(\rho_{\mathrm{cr}}^5 - \rho_{\mathrm{cr}}^4)^2}(\rho - \rho_{\mathrm{cr}}^4)^2 + \omega_{\max}), & \\ \quad \text{if } \rho_{\mathrm{cr}}^4 \le \rho < \rho_{\mathrm{cr}}^5, & \\ 0, & \text{if } \rho_{\mathrm{cr}}^5 \le \rho < \rho_{\mathrm{j}} \end{cases} \tag{11}$$

where λ, ξ are two random numbers in the interval $(-1, 1)$, $\varepsilon_{\max}, \omega_{\max}$ are maximum values, ρ_{cr}^i $(i = 1, 2, 3, 4, 5)$ is the critical value, ρ_{j} is the jam density. Note: λ, ξ can reflect the driver's individual difference, i.e. $\lambda \le 0, \xi \ge 0$ as for the aggressive drivers and $\lambda \ge 0, \xi \le 0$ as for the conservative drivers. In this paper, we do not study the quantitative effect that the stochastic property of the individual difference has on traffic flow, so we can here neglect some stochastic properties of the parameters λ, ξ (e.g., the average, variance, and probability distribution of λ, ξ) and will in the future use many observed data to calibrate the stochastic properties of λ, ξ and further explore the complex phenomena that are resulted by the driver's individual difference. In addition, the probability distribution has no qualitative impacts on the following results. Thus, we can assume that λ, ξ are uniform distributions whose average values are zero and we need not define λ, ξ as other distributions (e.g., normal distribution) in this paper. For simplicity, we here apply the Matlab function to randomly produce λ, ξ in the following numerical test. $\varepsilon_{\max}$ will first increase then decrease with the real density $\bar{\rho}$ in the real traffic system, so we for simplicity define them as follows:

$$\varepsilon_{\max} = \mu e^{-\frac{(\bar{\rho} - \rho_{\mathrm{cr}}^6)}{\sigma}}, \tag{12}$$

where μ, σ are two parameters, ρ_{cr}^6 is the critical value. In addition, we here assume that $\omega_{\max}$ is constant for simplicity.

In this paper, we here define the equilibrium speed as follows [37]:

$$v_{\mathrm{e}}(\rho) = v_{\mathrm{f}}\left(1 \Big/ \left(1 + \exp\left\{\frac{\rho/\rho_{\mathrm{j}} - 0.25}{0.06}\right\}\right) - 3.72 \times 10^{-6}\right), \tag{13}$$

where v_{f} is the free flow speed. The parameters in (5)–(13) have little qualitative effect on the following results, so we set them as follows:

$v_{\mathrm{f}} = 30$ m/s, $\rho_{\mathrm{j}} = 0.2$ veh/m, $\rho_{\mathrm{cr}}^1 = \rho_{\mathrm{cr}}^3 = 0.01$ veh/m, $\rho_{\mathrm{cr}}^2 = \rho_{\mathrm{cr}}^4 = 0.06$ veh/m, $\rho_{\mathrm{cr}}^5 = 0.1$ veh/m, $\rho_{\mathrm{cr}}^6 = 0.04$ veh/m, $\mu = 0.01, \sigma = 0.0001$, $\omega_{\max} = 0.1$.

Applying the above parameters, we can obtain the running speed and the real flow (see Figs. 4, 5 and 6). From the three figures, we have:

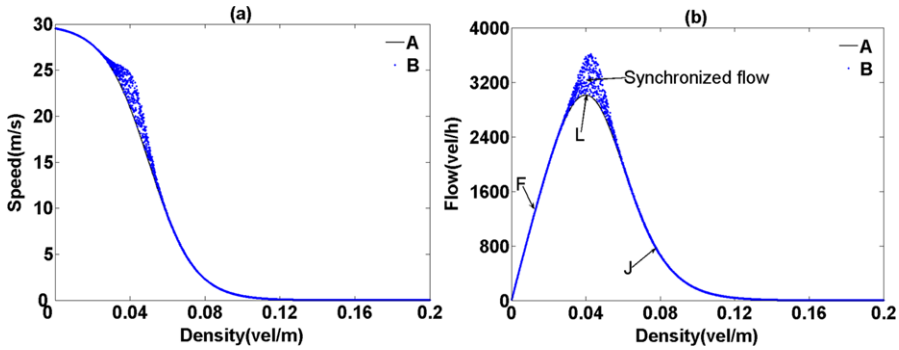

Fig. 4 The speed-density and flow-density relationships of equilibrium flow, where the curves "A" are the equilibrium speed-density and flow-density curves of the classical fundamental diagram theory and the widely scattered data "B" are the widely scattered speed-density and flow-density data when the traffic system only has the aggressive drivers

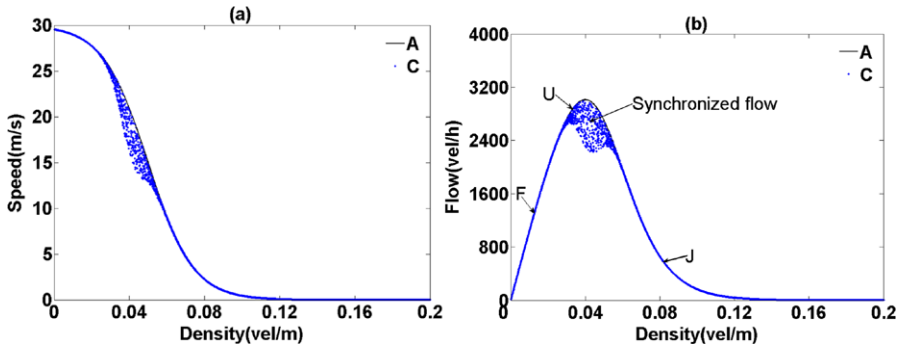

Fig. 5 The speed-density and flow-density relationships of equilibrium flow, where the widely scattered data "C" are the widely scattered speed-density and flow-density data when the traffic system only has the conservative drivers

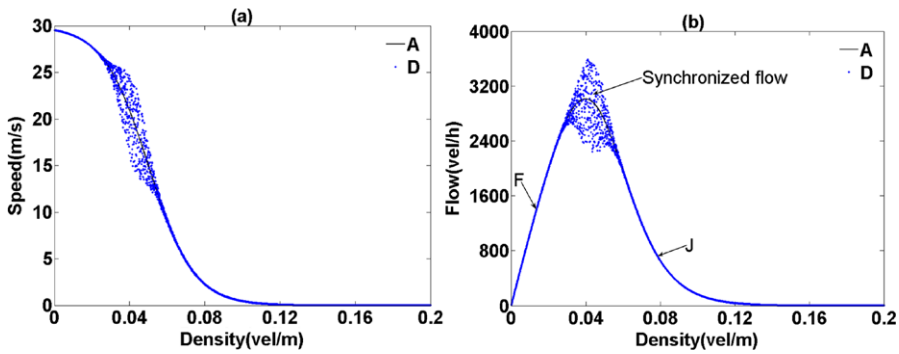

Fig. 6 The speed-density and flow-density relationships of equilibrium flow, where the widely scattered data "D" are the widely scattered speed-density and flow-density data when the traffic system simultaneously has the conservative and aggressive drivers

(1) The speed-density and flow-density data are divided into three different regions (see Figs. 4, 5 and 6). In the first region, the real density is very low; the running speed is approximately equal to the free flow speed and the real flow approximately linearly increases with the real density; the speed-density and flow-density data are scattered around the equilibrium speed-density and flow-density curves, where the widths of these scattered data are very narrow and slightly increase with the real density, i.e., the scattered data appear as two thicker lines. In the second region, the real density is moderate, the speed-density and flow-density data is scattered widely in a two-dimensional region. In the third region, the real density is very high, the scattered speed-density and flow-density data appear but quickly degenerate into the equilibrium speed-density and flow-density.

(2) When the traffic system only has the aggressive drivers, the speed-density and flow-density

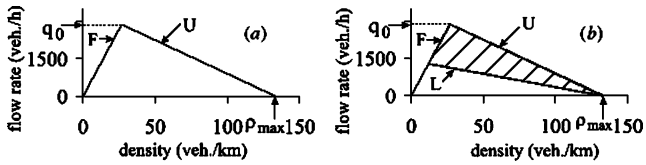

Fig. 7 The boundary lines in the fundamental diagram theory and the three phase traffic flow theory [15]

data are both above the equilibrium speed-density and flow-density curves (see Fig. 4); when the traffic system only has the conservation drivers, the speed-density and flow-density data are both under the equilibrium speed-density and flow-density curves (see Fig. 5); when the traffic system simultaneously has the aggressive and conservative drivers, the speed-density and flow-density data bestride the equilibrium speed-density and flow-density curves (see Fig. 6). These results further show that the aggressive drivers will enhance the running speed and real flow and the conservative drivers will reduce the running speed and real flow.

(3) When the real density is very low, ε, η have little effect on the running speed and real flow. The running speed is approximately equal to the free flow speed while the real flow approximately linearly increases with the real density and there is little prominent difference between the aggressive and conservative drivers (see Figs. 4, 5 and 6).

(4) ε, η have great effects on the running speed and real flow when the real density is moderate. ε, η will produce some widely scattered data, i.e., the widely scattered data will be in a two-dimensional region but their widths are related to the driver's individual difference, i.e., the widths of these scattered data are the narrowest when the traffic system only has conservative drivers and the broadest when the traffic system simultaneously has the aggressive and conservative drivers (see Figs. 4, 5 and 6). In addition, the shapes of these scattered data are related to the properties of ε, η.

(5) When the real density is very high, ε, η have some effects on the running speed and real flow. At this time, the scattered speed-density and flow-density data appear but quickly degenerate into the equilibrium speed-density and flow-density curves. In addition, there is little prominent difference between the aggressive and conservative drivers (see Figs. 4, 5 and 6).

(6) The above results are qualitatively accordant with the analytical results and the real traffic, which show that the new fundamental diagram theory can be used to describe the complex traffic phenomena resulted by the driver's individual difference.

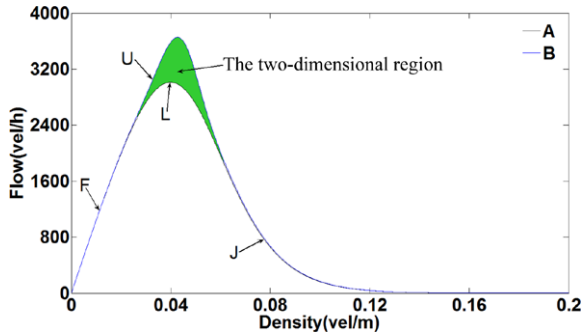

Fig. 8 The boundary line of the flow-density relationship, where the curves A and B are the same as those of Fig. 4

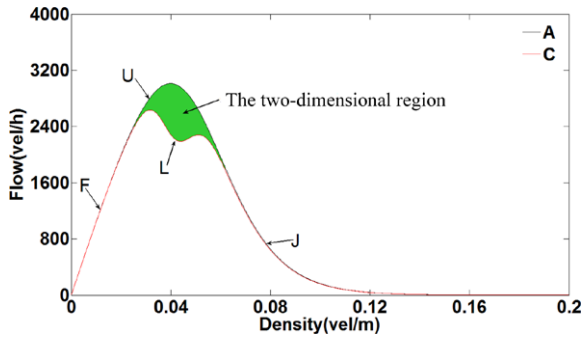

Fig. 9 The boundary line of the flow-density relationship, where the curves A and C are the same as those of Fig. 5

There are F-line, U-line, and L-line in three phase traffic flow theory [15] (see Fig. 7), so we next use the new fundamental diagram theory to study the effects of ε, η on the three lines (see Figs. 8, 9 and 10). From the three figures, we have:

(a) The new fundamental diagram theory also has F-line, L-line, and U-line (see Figs. 8, 9 and 10). When the real density is very low, there is little difference between the F-line of the new fundamental diagram theory and that of the classical

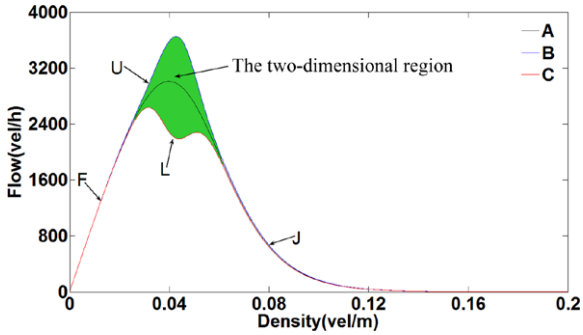

Fig. 10 The boundary line of the flow-density relationship, where the curves A, B, and C are the same as those of Figs. 4, 5 and 6

fundamental diagram theory, which further shows that ε, η have little effect on the running speed and real flow; when the real density is very high, the L-line and U-line will evolve into the same curve (we still call it the J-line); when the real density is moderate, the L-line and the U-line will form into a two-dimensional region, and the running speed and real flow are scattered widely in the two-dimensional region.

(b) If the traffic system only has the aggressive drivers, the L-line is the U-line of the classical fundamental diagram theory (see Fig. 8); if the traffic system only has the conservative drivers, the L-line is the U-line of the classical fundamental diagram theory (see Fig. 9); if the traffic system simultaneously has the aggressive and conservative drivers, the U-line is the U-line of Fig. 8 and the L-line is the L-line of Fig. 9 (see Fig. 10). This further shows that the aggressive drivers can enhance the running speed and real flow while the conservative drivers will reduce the running speed and real flow.

5 Conclusions

The three phase traffic flow theory and fundamental diagram theory have obtained many important results, but there are many drastic debates about whether they can perfectly reproduce or reasonably explain various complex traffic phenomena. Based on the driver's individual difference, we in this paper develop a new fundamental diagram theory with the drivers' perceived error and speed deviation difference. The analytical and numerical results show that the new fundamental diagram theory can reproduce the effects of the driver's perceived error and speed deviation difference on the equilibrium flow. These results are qualitatively accordant with the reality, which illustrate that the new fundamental diagram theory can better describe the real traffic flow than the existing fundamental diagram theories. In addition, the new fundamental diagram theory can help us to further explain why the widely scattered speed-density and flow-density data appear in the real traffic system and better understand the effects of the driver's individual difference on traffic flow.

6 Outlook

In this paper, we only study the qualitative impacts that the driver's perceived error and speed deviation difference have on equilibrium flow and do not further explore the effects of the driver's individual difference on nonequilibrium traffic flow. In addition, various stochastic properties of the driver's individual difference (the stochastic distribution functions of the driver's perceived error and speed deviation difference, their means and variances, etc.) are not explicitly considered. Therefore, we should in the future develop more exact models and apply many observed data and specific spatiotemporal congestion patterns to further investigate various complex traffic phenomena resulted by the driver's individual difference.

Acknowledgements This study has been supported by the Program for New Century Excellent Talents in University, China (No. NCET-08-0038), the National Natural Science Foundation of China (Nos. 70971007 and 70821061).

References

1. Chowdhury, D., Santen, L., Schreckenberg, A.: Statistics physics of vehicular traffic and some related systems. Phys. Rep. **329**, 199–329 (2000)
2. Kerner, B.S.: Three-phase traffic theory and highway capacity. Physica A **333**, 379–440 (2004)
3. Kerner, B.S., Rehborn, H.: Experimental features and characteristic of traffic jams. Phys. Rev. E **53**, R1297–R1300 (1996)
4. Kerner, B.S., Rehborn, H.: Experimental properties of complexity in traffic flow. Phys. Rev. E **53**, R4275–R4278 (1996)

5. Kerner, B.S., Rehborn, H.: Experimental properties of phase transitions in traffic flow. Phys. Rev. Lett. **79**, 4030–4033 (1997)
6. Kerner, B.S., Klenov, S.L., Konhäuster, P.: Asymptotic theory of traffic jams. Phys. Rev. E **56**, 4200–4216 (1997)
7. Kerner, B.S.: Experimental features of self-organization in traffic flow. Phys. Rev. Lett. **81**, 3797–3800 (1998)
8. Kerner, B.S.: A theory of congested traffic flow. In: Proceedings of the 3rd International Symposium on Highway Capacity, Road Directorate, Denmark, vol. 2, pp. 621–642 (1998)
9. Kerner, B.S.: Congested traffic flow: observation and theory. Transp. Res. Rec. **1678**, 160–167 (1999)
10. Kerner, B.S.: Experimental features of the emergence of moving jams in free traffic flow. J. Physics A **33**, L221–L228 (2000)
11. Kerner, B.S.: Theory of breakdown phenomena at highway bottlenecks. Transp. Res. Rec. **1710**, 136–144 (2000)
12. Kerner, B.S.: Empirical features of congested patterns at highway bottlenecks. Transp. Res. Rec. **1802**, 145–154 (2002)
13. Kerner, B.S.: Empirical macroscopic features of spatio-temporal traffic pattern at highway bottlenecks. Phys. Rev. E **65**, 046138 (2002)
14. Kerner, B.S., Klenov, S.L.: A microscopic model for phase transition in traffic flow. J. Physics A **35**, L31–L43 (2002)
15. Kerner, B.S., Klenov, S.L., Wolf, D.E.: Cellular automata approach to three-phase traffic theory, J. Physics A **35**, 9971–10013 (2002)
16. Kerner, B.S., Klenov, S.L.: Microscopic theory of spatial-temporal congested traffic patterns at highway bottlenecks. Phys. Rev. E **68**, 036130 (2003)
17. Kerner, B.S.: The Physics of Traffic. Springer, Heidelberg (2004)
18. Kerner, B.S., Rehborn, H., Aleksic, M., Haug, A.: Recognition and tracking of spatial-temporal congested traffic patterns on freeways. Transp. Res. C **12**, 369–400 (2004)
19. Kerner, B.S.: Control of spatialtemporal congested traffic patterns at highway bottleneck. Physica A **355**, 565–601 (2005)
20. Kerner, B.S.: Microscopic three-phase traffic theory and its application for freeway traffic control. In: Proceeding of International Symposium on Transportation and Traffic Theory, pp. 181–203. Elsevier, Amsterdam (2005)
21. Kerner, B.S., Klenov, S.L., Hiller, A., Rehborn, H.: Microscopic features of moving traffic jams. Phys. Rev. E **73**, 046107 (2006)
22. Kerner, B.S., Klenov, S.L.: Probabilistic breakdown phenomenon at on-ramp bottlenecks in three-phase traffic theory: congestion nucleation in spatially non-homogeneous traffic. Physica A **364**, 473–492 (2006)
23. Kerner, B.S.: On-ramp metering based on three-phase traffic theory. Traffic Eng. Control **48**, 28–35 (2007)
24. Kerner, B.S.: Phase transition in traffic flow on multilane roads. Phys. Rev. E **80**, 056101 (2009)
25. Kerner, B.S.: Introduction to Modern Traffic Flow Theory and Control. Springer, Berlin (2009)
26. Gupta, A.K., Katiyar, V.K.: Phase transition of traffic states with on-ramp. Physica A **371**, 674–682 (2006)
27. Davis, L.C.: Driver choice compared to controlled diversion for a freeway double on-ramp in the framework of three-phase traffic theory. Physica A **387**, 6395–6410 (2008)
28. Gao, K., Jiang, R., Wang, B.H., Wu, Q.S.: Discontinuous transition from free flow to synchronized flow induced by short-range interaction between vehicles in three-phase traffic flow model. Physica A **388**, 3233–3243 (2009)
29. Tian, J.F., Jia, B., Li, X.G., Jiang, R., Zhao, X.M., Gao, Z.Y.: Synchronized traffic flow simulating with cellular automaton model. Physica A **388**, 4827–4837 (2009)
30. Huang, D.W.: How the on-ramp inflow causes bottleneck. Physica A **388**, 63–70 (2009)
31. Zhao, B.H., Hu, M.B., Jiang, R., Wu, Q.S.: A realistic cellular automaton model for synchronized traffic flow. Chin. Phys. Lett. **26**, 118902 (2009)
32. He, S., Guan, W., Song, L.: Explaining traffic patterns at on-ramp vicinity by a driver perception model in the framework of three-phase traffic theory. Physica A **389**, 825–836 (2010)
33. Lighthill, M.J., Whitham, G.B.: On kinematic waves II: a theory of traffic on long crowded roads. Proc. R. Soc. Lond. Ser. A **229**, 317–345 (1955)
34. Richards, P.I.: Shock waves on the highway. Oper. Res. **4**, 42–51 (1956)
35. Payne, H.J.: Models of freeway traffic and control. In: Bekey, G.A. (ed.) Mathematical Models of Public System. Simulation Councils Proceedings Series, vol. 1, pp. 51–61 (1971)
36. Gazis, D.C., Herman, R.: The moving and "phantom" bottlenecks. Transp. Sci. **26**, 223–229 (1992)
37. Kerner, B.S., Konhäuster, P.: Cluster effect in initial homogeneous traffic flow. Phys. Rev. E **48**, R2335–R2338 (1993)
38. Daganzo, C.F.: The cell transmission model: a dynamic representation of highway traffic consistent with the hydrodynamic theory. Transp. Res. B **28**, 269–287 (1994)
39. Bando, M., Hasebe, K., Nakayama, A., Shibata, A., Sugiyama, Y.: Dynamical model of traffic congestion and numerical simulation. Phys. Rev. E **51**, 1035–1042 (1995)
40. Helbing, D.: Improved fluid-dynamic model for vehicular traffic. Phys. Rev. E **51**, 3164–3169 (1995)
41. Helbing, D.: Gas-kinematic derivation of Navier-Stokes-like traffic equations. Phys. Rev. E **53**, 2366–2381 (1996)
42. Wagner, C., Hoffmann, C., Sollacher, R., Wagenhuber, J., Schürmann, B.: Second-order continuum traffic flow model. Phys. Rev. E **54**, 5073–5085 (1996)
43. Daganzo, C.F.: A continuum theory of traffic dynamics for freeways with special lanes. Transp. Res. B **31**, 83–102 (1997)
44. Daganzo, C.F., Li, W.H., Castillo, J.M.: A simple physical principle for the simulation of freeways with special lanes and priority vehicles. Transp. Res. B **31**, 103–125 (1997)
45. Holland, E.N., Woods, A.W.: A continuum model for dispersion of traffic on two-lane roads. Transp. Res. B **31**, 473–485 (1997)
46. Zhang, H.M.: A theory of nonequilibrium traffic flow. Transp. Res. B **32**, 485–498 (1998)
47. Helbing, D., Treiber, M.: Numerical simulation of macroscopic traffic equations. Comput. Sci. Eng. **1**, 89–99 (1999)
48. Hebling, D., Hennecke, A., Treiber, M.: Phase diagram of traffic states in the presence of inhomogeneities. Phys. Rev. Lett. **82**, 4360–4363 (1999)

49. Shvetsov, V., Helbing, D.: Macroscopic dynamics of multilane traffic. Phys. Rev. E **59**, 6328–6339 (1999)
50. Treiber, M., Hennecke, A., Helbing, D.: Derivation, properties, and simulation of a gas-kinematic-based, non-local traffic model. Phys. Rev. E **59**, 239–253 (1999)
51. Aw, A., Rascle, M.: Resurrection of "second-order" models of traffic flow. SIAM J. Appl. Math. **60**, 916–938 (2000)
52. Treiber, M., Hennecke, A., Helbing, D.: Congested traffic states in empirical observations and microscopic simulations. Phys. Rev. E **62**, 1805–1824 (2000)
53. Nelson, P.: Synchronized traffic flow from a modified Lighthill-Whitham model. Phys. Rev. E **61**, R6052–R6055 (2000)
54. Helbing, D.: Traffic and related self-driven many-particle systems. Rev. Mod. Phys. **73**, 1067–1141 (2001)
55. Helbing, D., Hennecke, A., Shvetsov, V., Treiber, M.: MASTER: macroscopic traffic simulation based on a gas-kinematic, non-local traffic model. Transp. Res. B **35**, 183–211 (2001)
56. Wong, G.C.K., Wong, S.C.: A multi-class traffic flow model-an extension of LWR model with heterogeneous drivers. Transp. Res. A **36**, 827–841 (2002)
57. Jiang, R., Wu, Q.S., Zhu, Z.J.: A new continuum model for traffic flow and numerical tests. Transp. Res. B **36**, 405–419 (2002)
58. Munoz, J.C., Daganzo, C.F.: Moving bottlenecks: a theory grounded on experimental observation. In: Proceeding of the 15th International Symposium of Traffic and Transportation Theory, pp. 441–462. Pergamon, Oxford (2002)
59. Aw, A., Klar, A., Materne, T., Rascle, M.: Derivation of continuum traffic flow models from microscopic follow-the-leader models. SIAM J. Appl. Math. **63**, 259–278 (2002)
60. Zhang, H.M.: A nonequilibrium traffic model devoid of gas-like behavior. Transp. Res. B **36**, 275–290 (2002)
61. Xue, Y., Dai, S.Q.: Continuum traffic model with the consideration of two delay scales. Phys. Rev. **68**, 066123 (2003)
62. Helbing, D.: A section-based queueing-theoretical traffic model for congestion and travel time analysis in networks. J. Physics A **36**, L593–L598 (2003)
63. Benzoni-Gavage, S., Colombo, R.: An n-populations model for traffic flow. Euro. J. Appl. Math. **14**, 587–612 (2003)
64. Tang, T.Q., Huang, H.J., Gao, Z.Y.: Stability of the car-following model on two lanes. Phys. Rev. E **72**, 066124 (2005)
65. Ossen, S.J., Hoogendoorn, S.P.: Car-following behavior analysis from microscopic trajectory data. Transp. Res. Rec. **1934**, 13–21 (2005)
66. Nagel, K., Nelson, P.: A critical comparison of the kinematic-wave model with observational data. In: Proceeding of the 15th International Symposium of Traffic and Transportation Theory, pp. 145–163. Elsevier, Amsterdam (2005)
67. Treiber, M., Kesting, A., Helbing, D.: Delays, inaccuracies and anticipation in microscopic traffic models. Physica A **360**, 71–88 (2006)
68. Huang, H.J., Tang, T.Q., Gao, Z.Y.: Continuum modeling for two-lane traffic flow. Acta Mech. Sin. **22**, 131–137 (2006)
69. Gupta, A.K., Katiyar, V.K.: A new multi-class continuum model for traffic flow. Transportmetrica **3**, 73–85 (2007)
70. Helbing, D., Tilch, B.: A power law for the duration of high-flow states and its interpretation from heterogeneous traffic flow perspective. Eur. Phys. J. B **68**, 577–586 (2009)
71. Helbing, D.: Derivation of non-local macroscopic traffic equations and consistent traffic pressures from microscopic car-following models. Eur. Phys. J. B **69**, 539–548 (2009)
72. Treiber, M., Kesting, A., Helbing, D.: Understanding widely scattered traffic flows, the capacity drop, and platoons as effects of variance-driven time gaps. Phys. Rev. E **74**, 016123 (2006)
73. Schönhof, M., Helbing, D.: Empirical features of congested traffic states and their implications for traffic modeling. Transp. Sci. **41**, 135–166 (2007)
74. Schönhof, M., Helbing, D.: Criticism of three-phase traffic theory. Transp. Res. B **43**, 784–797 (2009)
75. Treiber, M., Kesting, A., Helbing, D.: Three-phase traffic theory and two-phase models with fundamental diagram in the light of empirical stylized facts. Transp. Rev. B **44**, 983–1000 (2010)
76. Ngoduy, D.: Multiclass first order modelling of traffic networks using discontinuous flow-density relationships. Transportmetrica **6**, 121–141 (2010)
77. Bank, J.H.: Investigation of some characteristics of congested flow. Transp. Res. Rec. **1678**, 128–134 (1999)
78. Nishinari, K., Treiber, M., Helbing, D.: Interpreting the wide scattering of the synchronized traffic data by time gap statistics. Phys. Rev. E **68**, 067101 (2003)
79. Treiber, M., Helbing, D.: Macroscopic simulation of widely scattered synchronized traffic states. J. Physics A **32**, L17–L23 (1999)
80. Treiber, M., Helbing, D.: Memory effects in microscopic traffic models and wide scattering in flow-density data. Phys. Rev. E **68**, 046119 (2003)
81. Ngoduy, D.: Multiclass first-order traffic model using stochastic fundamental diagrams. Transportmetrica **7**, 111–125 (2011)
82. Yang, H.H., Peng, H.: Development of an errorable car-following driver model. Veh. Syst. Dyn. **48**, 751–773 (2010)
83. Li, J., Chen, Q.Y., Wang, Y., Ni, D.: Investigation of LWR model with flux function driven by random free flow speed. In: The 88th Transportation Research Board Annual Meeting, DVD-ROM, Washington, DC
84. Daganzo, C.F.: Requiem for second-order fluid approximations of traffic flow. Transp. Res. B **29**, 277–286 (1995)